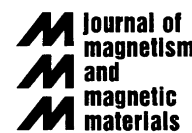




ELSEVIER

Journal of Magnetism and Magnetic Materials 226–230 (2001) 1688–1693



www.elsevier.com/locate/jmmm

# Layered magnetic structures: history, facts and figures

P. Grünberg\*

*Institute for Solid State Physics, Forschungszentrum Jülich- IFF, 52425 Jülich, Germany*

## Abstract

An overview is given of the most important properties of layered magnetic structures. Typical and record values for the strengths of the observed effects are compiled from the literature. The historical development and the most important applications are described. © 2001 Elsevier Science B.V. All rights reserved.

**Keywords:** Magnetic multilayers; Review

## 1. First experiments

The first experiment on thin magnetic films was performed by Kundt in 1884 who proved that there is a rotation of the polarization of light when it transmits ferromagnetic metals like Fe, Co or Ni [1]. It is clear that thin films required such experiments. Earlier, Faraday had seen this ‘Faraday rotation’ in a specimen of glass, subjected to a magnetic field. For almost a century the investigation of this effect became the main driving force for research in thin magnetic films. Kundt established the proportionality between the rotation and the magnetization component parallel to the light beam. This was called Kundt’s law, the proportionality factor being Kundt’s constant.

While Kundt used electrochemical deposition for the preparation of his films, due to the improvements in vacuum techniques by 1950, thermal evaporation was favored which enabled research on a more reliable basis. As a result, in 1968, surface anisotropy (or more generally interface anisotropy) was seen for the first time experimentally [2,3], which had been already predicted by Néel in 1954 [4]. We turn now to a description of this and other interesting phenomena which were discovered up to now in layered magnetic structures.

## 2. Special anisotropies at surfaces and interfaces

Néel-type surface anisotropy is due to the symmetry breaking at a surface and can be predicted from data on bulk anisotropy and magnetostriction. This is not the only possibility. By extended numerical work of various theory groups, a relation between anisotropy and spin–orbit coupling and hence more generally with the electronic band structure could be established. Based on this, the appearance of strong perpendicular anisotropy in Co/Pd multilayers reported in 1985 [5] could be explained theoretically [6]. Since Ni has the same number of valence electrons as Pd, the calculations were extended to Co/Ni structures and it was predicted that a strong interface anisotropy with easy axis perpendicular to the sample plane should exist also at the Co/Ni interface. Indeed experiments on (Co1/Ni2)<sub>20</sub>-layered structures with a total thickness of 120 Å showed the strong perpendicular anisotropy, as predicted, orienting the magnetization spontaneously perpendicular to the sample plane [6].

In Table 1 we display values for the strength of interface anisotropy as defined by

$$\sigma_A = K_S \cos^2 \theta, \quad (1)$$

where  $\sigma_A$  is the areal energy density connected with the anisotropy, and the magnetization includes an angle  $\theta$  with the surface normal. Hence for negative  $K_S$ , minimum energy is obtained for  $\theta = 0$  and the normal to the sample plane is an easy axis.

The demagnetizing areal energy density, which favors the magnetization to be in the sample plane is  $0.5 \mu_0 M^2 t$ ,

\* Fax: + 49-2461-614443.

E-mail address: p.gruenberg@fz-juelich.de (P. Grünberg).

Table 1

Values for  $K_S$  as defined by Eq. (1), compiled from the literature [3,7,8]. The free surface is indicated by ‘UHV’

Interface	$K_S$ (mJ/m <sup>2</sup> )
Co/Pd	−0.92
Co/Pt	−1.15
Co/Ni	−0.42
Co/Au	−1.28
Ni/UHV	0.48
Ni/Cu	0.22
Fe/Ag	−0.79
Fe/Au	−0.54
Fe/UHV	−0.89

where  $M$  is the magnetization and  $t$  the thickness of the film. For a monolayer of Fe with  $t = 0.14$  nm we obtain  $0.53$  mJ/m<sup>2</sup>, hence by comparing the values in Table 1 we would expect, e.g. for the Fe/Au system, a spontaneous orientation of the magnetization perpendicular to the sample plane only in the limit of one monolayer of Fe. (The corresponding energy for a Fe monolayer due to an external field  $B = \mu_0 H = 0.1$  T is  $BMt = 0.025$  mJ/m<sup>2</sup>.)

Apart from choosing the right materials one can increase the influence of  $\sigma_A$  on the total anisotropy further by increasing the density of interfaces. This was brought to the extreme of alternating just one monolayer of Fe with one monolayer of Au or Pt in Ref. [9]. Saturation fields were around 2 T in the case of (Fe/Au)<sub>100</sub> films and more than 6 T in the case of (Fe/Pt)<sub>100</sub> (see Fig. 1).

In thin films the electronic properties are characterized by quantum-well states. This aspect of the dependence of surface anisotropy on electronic properties has also recently been demonstrated [10]. The surface anisotropy of a Co film oscillated and even changed sign as a function of the thickness of a Cu overlayer. This is clearly due to the quantum-well states in the Cu.

Another type, which can also be classified as interface anisotropy is the so-called ‘exchange anisotropy’ [11]. It was first seen in 1956 in fine Co particles, covered by antiferromagnetic Co-oxide but soon also reproduced in structures of thin films. By means of this effect, it is possible to shift hysteresis curves of samples on the field axis. An example is shown in Fig. 2 [11,12] for the so-called ‘spinvalve structure’. The ‘free’ layer remagnetizes in small fields, whereas the hysteresis curve of the ‘pinned’ layer is shifted to positive fields by the ‘exchange field’  $H_E$ . Fig. 2(c) shows the related GMR effect to be discussed below. We can use the related interface areal energy density, which we denote by  $\sigma_{ex}$ , for a description of the strength of the effect. The exchange field then is given by

$$H_E = \sigma_{ex} / (\mu_0 M_{FM} t_{FM}). \quad (2)$$

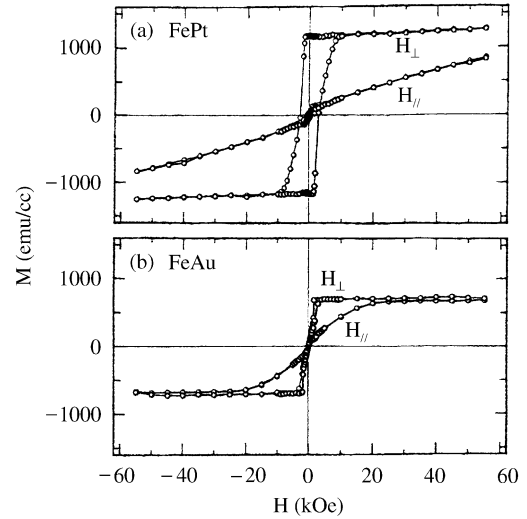


Fig. 1. Magnetization curves at room temperature as a function of applied field parallel ( $H_{\parallel}$ ) and perpendicular ( $H_{\perp}$ ) to the film plane of (a) a  $[\text{Fe}/\text{Pt}]_{100}$  film and (b) a  $[\text{Fe}/\text{Au}]_{100}$  film [9].

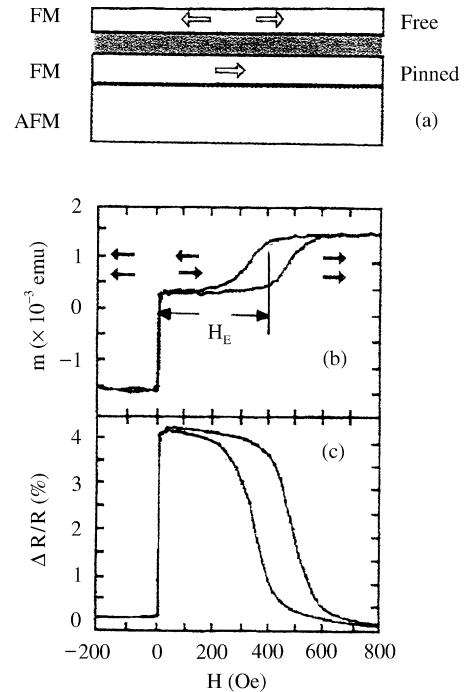


Fig. 2. (a) Schematic diagram of a spin-valve device. (b) Hysteresis loop  $m(H)$ , and (c) magnetoresistance,  $\Delta R/R(H)$ , of a  $6 \text{ nmFe}_{20}\text{Ni}_{80}/2.2 \text{ nmCu}/4 \text{ nmFe}_{20}\text{Ni}_{80}/7 \text{ nmFeMn}$  GMR spin valve at room temperature. From  $H_E$  as indicated and  $t_{FM} = 4$  nm,  $\mu_0 M_{FM} \approx 1$  T for permalloy we obtain from Eq. (2)  $\sigma_{ex} = 0.13$  mJ/m<sup>2</sup> [11,12].

Table 2

Strength of exchange anisotropy effect in terms  $\sigma_{\text{ex}}$  due to various AF materials (from Ref. [11])

Antiferromagnetic material	$\sigma_{\text{ex}}$ (mJ/m <sup>2</sup> )
Fe <sub>50</sub> Mn <sub>50</sub> (poly-ann)	0.05–0.47
Ni <sub>50</sub> Mn <sub>50</sub> (poly-ann)	0.16–0.46
NiO	0.05–0.29
CoO	0.14–0.48

Here  $M_{\text{FM}}$  and  $t_{\text{FM}}$  are, respectively, the magnetization and the thickness of the ferromagnetic film, adjacent to the antiferromagnet. In Table 2 some representative values for  $\sigma_{\text{ex}}$  are given.

### 3. Properties of ultrathin films: Curie point, magnetization, critical behavior

It is clear that research in ultrathin films requires extreme care with growth properties. Therefore, in the following, only a few representative examples will be discussed which seem to be reliable and representative [2,3].

As intuitively expected there is a reduction of  $T_{\text{C}}$  for decreasing film thickness. Systematic investigations of this aspect for Fe films showed that there can be an important difference depending on which crystallographic orientation is used. For the close-packed Fe-(110) monolayer on tungsten, we have  $T_{\text{C}} = 225$  K in the uncovered case and  $T_{\text{C}} = 282$  K for a film covered with Ag. A (100)-type monolayer, on the other hand, seems not to order magnetically. This is believed to be due to the fact that in such a monolayer the nearest neighbors of the corresponding bulk structure are missing. If we add the nearest neighbors, we arrive at a two-monolayer (100) Fe film with  $T_{\text{C}} = 220$  K which is close to the 225 K for the (110)-type monolayer where we have the nearest neighbors already for the monolayer.

The behavior of the saturation magnetization in ultrathin films, i.e. the value of their magnetization at low temperatures or moment per magnetic atom, was for a long time an open question both theoretically and experimentally. The situation changed due to the strong progress in first-principles self-consistent band theories and to the introduction of ‘conversion electron Mössbauer spectroscopy’ (CEMS), in addition to the conventional magnetometries. Today there is good evidence that magnetic moments in ultrathin films are more or less slightly changed — mostly enhanced — but this depends also on an adjacent nonmagnetic material. For example, in Ref. [9] an increase of the Fe moment from  $\mu = 2.2 \mu_{\text{B}}$  as measured in the bulk to  $\mu = 2.5 \mu_{\text{B}}$  for a monolayer of Fe embedded in Au is reported.

Among the properties of ultrathin magnetic films of great interest is also the critical behavior close to the Curie temperature  $T_{\text{C}}$ . It is related to the model by which we can describe the magnetic structure and the interactions which are responsible for the magnetic order. The main question is, whereupon lowering the film thickness, three-dimensional (3D)-type models change to two-dimensional (2D)-type ones.

Just below the Curie temperature, in the range of the onset of magnetic order the magnetization  $M$  is given by  $M \propto (1 - T/T_{\text{C}})^{-\beta}$ , where  $\beta$  is the so-called critical exponent. The value of  $\beta$  depends on the underlying model. It can be determined experimentally from careful measurement of  $M$  close to  $T_{\text{C}}$  and compared with the theory.

For thin films of Ni it was found that the crossover from 3D to 2D behavior occurs at a thickness around 6 monolayer (ML) [13]. The corresponding values of  $T_{\text{C}}$  are around 450 K which is close to 70% of  $T_{\text{C}} = 630$  K of bulk Ni. For bulk Fe and Co the Curie points are at 1043 and 1388 K, respectively. Hence the  $T_{\text{C}}$  values corresponding to the crossover region are expected to be above 700 K. If one were to do such an experiment, one would have to deal strongly with the problem of interdiffusion between film and substrate or clustering of the film material. That is why the transition region for the critical exponents so far has only been determined for thin Ni films.

### 4. Interlayer exchange coupling (IEC)

Already in 1958 Néel [14] predicted that dipolar fields due to interface corrugations could lead to effective ferromagnetic interlayer coupling, trying to align the magnetizations parallel. The effect was called ‘orange peel coupling’ and has probably been observed in many cases, although it is generally difficult to trace the origin of ferromagnetic-type coupling, because there is always the possibility that it is due to pinholes and ferromagnetic bridges. This is different when the coupling leads to noncollinear alignment, like the coupling which was reported in 1986 for Dy and Gd films separated by Y interlayers and for Fe films separated by Cr interlayers [15,16].

For transition metal ferromagnets separated by paramagnetic interlayers, the coupling is phenomenologically described by the connected areal energy density  $\sigma_{\text{IEC}}$ , via

$$\sigma_{\text{IEC}} = -J_1 \cos \theta - J_2 (\cos \theta)^2. \quad (3)$$

Here  $\theta$  is the angle between the magnetizations of the films on both sides of the spacer layer. The parameters  $J_1$  and  $J_2$  describe the type and the strength of the coupling. If the term with  $J_1$  dominates, then from the minima of Eq. (3) the coupling is ferro (antiferro)-magnetic for positive (negative)  $J_1$ . If the term with  $J_2$

Table 3  
Selection of observed coupling strengths and periods [15,16]

Sample	Maximum strength in mJ/m <sup>2</sup> at (thickness) in nm	Periods in ML and (nm)
Co/Cu/Co (100)	0.4 (1.2)	2.6 (0.47), 8 (1.45)
Co/Cu/Co (110)	0.7 (0.85)	9.8 (1.25)
Co/Cu/Co (111)	1.1 (0.85)	5.5 (1.15)
Fe/Au/Fe (100)	0.85 (0.82)	2.5 (.51), 8.6 (1.75)
Fe/Cr/Fe (100)	> 1.5 (1.3)	2.1 (0.3), 12 (1.73)
Fe/Mn/Fe (100)	0.14 (1.32)	2 (0.33)
Co/Ru (0001)	6 (0.6)	5.1 (1.1)
Co/Rh/Co (111)	34 (0.48)	2.7 (0.6)
Co/Os (111-text'd)	0.55 (0.9)	7 (1.5)
Co/Ir (111)	2.05 (0.5)	4.5 (1.0)

dominates and is negative we obtain 90°-coupling. The first term of Eq. (3) is often called bilinear coupling and the second the biquadratic coupling.

Biquadratic coupling is thought to be mainly due to interface roughness and will not be further considered here. Bilinear coupling, on the other hand, is believed to be due to an indirect exchange interaction mediated by the conduction electrons of the spacer layer. It is closely related to the Ruderman–Kittel–Kasuya–Yoshida (RKKY) interaction, between localized moments mediated by the conduction electrons of a host metal. A more detailed consideration shows that the oscillation periods of  $J_1$  as a function of the interlayer thickness are related to certain distances  $Q_i$ , that are critical spanning vectors of the Fermi surface of the interlayer material [15,16]. Observed values for  $J_1$  and the periods are quoted in Table 3.

The strength of the coupling depends on many details of the participating Fermi surfaces. It is now believed that materials from the same column of the periodic table should yield particularly large coupling strengths. This can be explained on the basis of favorable band matching [17]. The record value found for the Co/Rh combination (see Table 3) seems to support this concept.

## 5. Giant magnetoresistance (GMR)

In magnetic multilayers the resistivity, both for currents parallel and perpendicular to the sample plane, has been found to depend on the relative magnetic alignment of the ferromagnetic films separated by the interlayers [18]. For the normal effect, the resistivity is highest for antialignment but there can also be an ‘inverse effect’, where this is reversed. The AF alignment can be provided by AF interlayer exchange or e.g. by hysteresis effects.

Since GMR was first seen in the exchange-coupled Fe/Cr structures it was assumed that there is a close

connection between coupling and GMR. Later various research groups found independently that it could also be seen in uncoupled layers. It was only important that the relative angle between the magnetizations in adjacent films could be varied, for example via hysteresis effects. Hence experimentally it seemed now that IEC and GMR are independent effects. Meanwhile the situation has changed again and a correlation between IEC and GMR has been established both theoretically and experimentally.

This is due to a theoretical description, invented by Slonczewski [19] which uses ‘spin currents’ for an explanation. A very interesting result of this theory is the possibility to use currents between the magnetic layers to switch their magnetization, via a current-induced coupling. It has recently been verified experimentally [20].

The GMR effect has been investigated in two different geometries, namely the current in plane (‘CIP’) and the current perpendicular plane (‘CPP’) geometries. The relative effect is stronger in the CPP geometry as compared to the CIP geometry but without special structuring, due to the extremely unfavorable situation (lateral dimensions some orders of magnitude larger than film thickness) the voltage drop perpendicular to the layers, in the CPP geometry, is very difficult to detect. On the other hand by structuring, GMR in CPP geometry can become sufficiently strong to be of interest even for the application (see the last section). Representative and record values for the GMR effect both in the CIP and the CPP geometry have been compiled in Table 4. Current efforts to increase the effect in the case of double layers include slight oxidation of the outer surfaces which is believed to lead to smoothening and increase of the electron specular reflection [25].

## 6. Tunnel magnetoresistance (TMR)

The basic TMR configuration, consists of two ferromagnetic films, separated by an insulating or semiconducting interlayer. The tunnel resistance depends on the relative angle between the magnetizations of the two ferromagnetic films and for the normal TMR effect, it is lowest (highest) for alignment (antialignment). For the inverse effect, which can also be observed, this situation is reversed. Julliere [31] who performed the first experiment in 1975, observed the normal effect and obtained maximum conductivity changes of 14% at low temperatures ( $\leq 4.2$  K). During the tunnelling process the electron spin was assumed to be conserved. This led to the well-known and frequently applied relation

$$\Delta R/R = (R_{AP} - R_P)/R_{AP} = 2P_1 P_2 / (1 + P_1 P_2) \quad (4)$$

for the relative change  $\Delta R$  of the resistance  $R$  when the magnetizations are switched from parallel to antiparallel.

Table 4

GMR: values for  $\Delta R/R$  which are representative of particularly strong effects or those used in sensors. Geometry is CIP unless specially marked with CPP

Sample	$\Delta R/R$ (%)	Temperature (K)	References
[Fe(4.5)/ Cr(12)] <sub>50</sub>	220	1.5	[21]
[Co(15)/ Cu(9)] <sub>30</sub>	42	300	
[Co(15)/ Cu(9)] <sub>30</sub>	78	4.2	[22]
[Co(8)/ Cu(8.3)] <sub>60</sub>	48	300	
[Co(10)/Cu(10)] <sub>100</sub>	115	4.2	[23]
[Co(10)/Cu(10)] <sub>100</sub>	65	300	
[Co(10)/Cu(10)] <sub>100</sub>	80	300	[24]
Co(25)/Cu(19)/Co(4)/Cu(19)/Co(25)	23.4	300	[25]
Co(3)/Cu(19)/Co(25)	17	300	[25]
Co <sub>90</sub> Fe <sub>10</sub> (40)/Cu(25)/Co <sub>90</sub> Fe <sub>10</sub> (8)...	7	300	[26]
NiFe(100)/Cu(25)/Co(22)	4.6	300	[27]
[CoNiFe/Cu] <sub>4-6</sub>	10–20	300	[28]
Fe(60)Co(8)/Cu(23)/AAF/Cu(23)/Co(8)Fe(60)	6	300	[29]
[Co(15)/Cu(12)] <sub>n</sub>	170	4.2	CPP [30]
[Co(12)/Cu(11)] <sub>180</sub>	55	300	CPP [30]

Here  $R_{AP}$  and  $R_P$  are the resistances in the antiparallel and parallel states, respectively, and  $P_1$  and  $P_2$  are the electron spin polarizations of the two electrodes. Basically this formula up to now is not questioned but there is a strong controversy as to how the relevant values for  $P_1$  and  $P_2$  can be obtained.

Fig. 3 displays TMR curves which are representative for the current state of the art. Record values of 40% and more have been obtained at room temperature [32,33].

From Eq. (5) it is clear that the normal (inverse) effect is observed if the spin polarizations at the two interfaces have the same (opposite) sign. Hence if a reference system with a known sign of polarization is used at one interface, the sign of polarization at the other interface can be determined.

De Teresa et al. [34] used as reference system  $\text{La}_{0.7}\text{Sr}_{0.3}\text{MnO}_3$  which both from theory as well as from photoemission experiments at low temperatures, has positive spin polarization. With this they confirmed that the effective spin polarization at the  $\text{Co}/\text{Al}_2\text{O}_3$  interface is positive as found before from F/I/S junctions where F is the ferromagnetic metal — here Co —, I denotes the insulating barrier, and S is a superconductor. (The F/I/S experiments for a long time had been the standard method to determine the absolute value of the relevant polarization at the F/I interfaces [35].) A positive polarization at  $E_F$  of Co contradicts the assumption that it can be predicted from the spin split density of states of the bulk material which would yield negative polarization. On the other hand, it was found that the effective spin polarization of Co is negative for the  $\text{Co}/\text{SrTiO}_3$  and  $\text{Co}/\text{Ce}_{0.69}\text{La}_{0.31}\text{O}_{1.845}$  interfaces, which shows that it depends also on the barrier material. In summary, it is

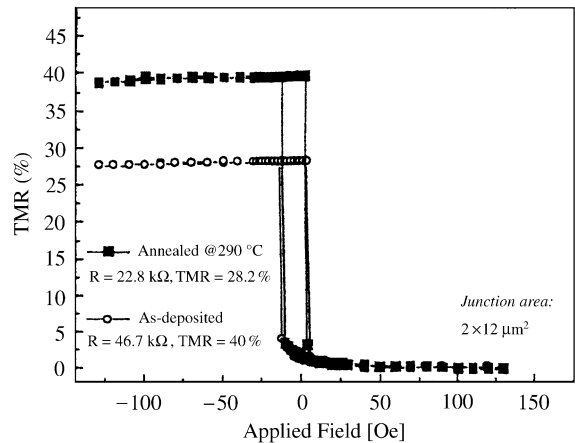


Fig. 3. TMR in  $\text{Co}_{82}\text{Fe}_{18}(3\text{ nm})/\text{Al}_2\text{O}_3/\text{Co}_{82}\text{Fe}_{18}/(4\text{ nm})\text{Mn}_{74}\text{Ir}_{16}$  structures [33].

now believed that spin polarizations are related to interface states which play also a major role in chemical bonding at the interfaces. The states relevant for TMR obviously are evanescent. This implies that the decay length of these states, which is related to the band structure of the barrier material has also to be included in the theory.

## 7. Applications

Layered magnetic structures are mainly useful for storage media and for sensors in data storage technology, as can be seen from the following time table:

1955: Proposal to use patches of permalloy films for magnetic random access memories (MRAMs) in computers. This failed at that time because of the appearance of ‘dynamic random access memories’ (DRAMs), based on semiconductors.

1958: Proposal to use thin films of MnBi for magneto-optic recording.

1973: Introduction of rare earth-transition metal (RE-TM) films for magneto-optic recording (are still in use today).

1979: IBM introduces thin-film technology for heads in hard disks. (Both the write and read processes were still inductive but the coil was made using thin film technology).

1991: Introduction of anisotropic magnetoresistance (AMR) effect, using permalloy films, for sensors in hard disks drives (HDD) by IBM.

1997: Introduction of GMR for the sensors in HDD, by IBM.

Other possible applications lie in robotics and sensors to control mechanical movements, e.g. in cars. In these sensors IEC has also found an application, where it is exploited in ‘artificial antiferromagnets (AAF)’. For this application the AFM in Fig. 2 would be replaced by an AAF.

The miniaturization aspect and the sensitivity of GMR are also of interest for galvanic separation in signal processing which so far has been the domain of optocouplers. Instead of converting an electrical signal into an optical one, one can use directly the fields produced by the currents together with GMR-type sensors and realize galvanic separation by means of magnetocouplers. Furthermore GMR in conjunction with magnetostrictive materials can also be used for pressure sensors [36].

Currently, both GMR and TMR are considered for applications in sensors and in MRAMs. Very recently Prinz [37] has proposed to use GMR in the CPP configuration for the MRAM application.

## 8. Final remark

Research on magnetic film structures has contributed to a better understanding of interactions in magnetism and magnetotransport. Most effects have found interesting applications. The preparation of these structures also has had a strong impact on studies of growth and structure. The most celebrated result in this context is probably the study of oscillatory coupling across Cr used as substrate the almost perfect surface of an Fe whisker [15,16]. Under these conditions it was possible to fabricate for the first time Cr interlayers which support the incommensurate spin density wave (ISDW), typical for almost perfect Cr. It is well known that the ISDW is extremely sensitive to imperfections. It remains a chal-

lenge to produce films of similar quality on conventional semiconducting or insulating substrates.

## References

- [1] A. Kundt, *Wied. Ann.* 23 (1884) 228.
- [2] U. Gradmann, in: K.H. Buschow (Ed.), *Handbook of Magnetic Materials*, Vol. 7, Elsevier, Amsterdam, 1993.
- [3] H.J. Elmers, *Int. J. Mod. Phys.* 19 (1995) 3115.
- [4] L. Néel, *J. Phys. Radium* 15 (1954) 225.
- [5] P.F. Carcia, A.D. Meinhaldt, A. Suna, *Appl. Phys. Lett.* 47 (1985) 178.
- [6] G.H.O. Daalderop, P.J. Kelly, F.J.A. den Broeder, *Phys. Rev. Lett.* 68 (1992) 682.
- [7] G.H.O. Daalderop et al., in: *Ultrathin Magnetic Structures I*, J.A.C. Bland, B. Heinrich (Eds.), Springer, Berlin, 1994.
- [8] W.J.M. de Jonge et al., in: *Ultrathin Magnetic Structures I*, J.A.C. Bland, B. Heinrich (Eds.), Springer, Berlin, 1994.
- [9] S. Mitani, K. Takanashi, H. Nakajima, K. Sato, R. Schreiber, P. Grünberg, H. Fujimori, *J. Magn. Magn. Mater.* 156 (1996) 7.
- [10] W. Weber et al., *Phys. Rev. Lett.* 18 (1996) 3424.
- [11] J. Nogues, I. Schuller, *J. Magn. Magn. Mater.* 192 (1999) 203.
- [12] B. Dieny, *J. Magn. Magn. Mater.* 136 (1994) 335.
- [13] Yi. Li, K. Baberschke, *Phys. Rev. Lett.* 68 (1992) 1208.
- [14] L. Néel, *Comptes Rendus* 255 (1962) 1545, 1676.
- [15] D. Bürgler, S.O. Demokritov, P. Grünberg, M.T. Johnson, in: K.H.J. Buschow (Ed.), *Handbook of Magnetic Materials*, Elsevier, Amsterdam, to appear.
- [16] P. Grünberg, D. Pierce, *Encyclopedia of Materials: Science and Technology*, 2001, Elsevier, Amsterdam, to appear.
- [17] J. Mathon, M. Villeret, D.M. Edwards, R.B. Muniz, *J. Magn. Magn. Mater.* 121 (1993) 242.
- [18] A. Fert, *Encyclopedia of Materials: Science and Technology*, 2001, Elsevier, Amsterdam, to appear.
- [19] J.C. Slonczewski, *J. Magn. Magn. Mater.* 159 (1996) L1.
- [20] J.A. Katine, F.J. Albert, R.A. Buhrman, C.B. Myers, D.C. Ralph, *Phys. Rev. Lett.* 84 (2000) 3149.
- [21] R. Schad et al., *Appl. Phys. Lett.* 64 (1994) 3500.
- [22] D.H. Mosca et al., *J. Magn. Magn. Mater.* 94 (1991) L1.
- [23] S.S.P. Parkin et al., *Appl. Phys. Lett.* 58 (1991) 2710.
- [24] H. Kano et al., *Appl. Phys. Lett.* 63 (1993) 2839.
- [25] W.F. Egelhoff et al., *J. Appl. Phys.* 79 (1996) 5277.
- [26] K.M.H. Lenssen et al., *J. Appl. Phys.* 85 (1999) 5531.
- [27] Ch. Tsang et al., *IEEE Trans. Magn.* 30 (1994) 3801.
- [28] J. Daughton et al., *IEEE Trans. Magn.* 30 (1994) 4608.
- [29] W. Clemens et al., *J. Appl. Phys.* 81 (1997) 4310.
- [30] M.A.M. Gijs, G.E.W. Bauer, *Adv. in Phys.* 46 (1997) 285.
- [31] M. Julliere, *Phys. Lett. A* 54 (1975) 225.
- [32] S.S.P. Parkin et al., *J. Appl. Phys.* 85 (1999) 5828.
- [33] S. Cardoso et al., *IEEE Trans. Magn.* 35 (1999) 2952.
- [34] J.M. de Teresa, A. Barthelemy, A. Fert, J.P. Contour, F. Montaigne, *Science* 286 (1999) 507.
- [35] C.T. Tanaka, J. Nowak, J. Moodera, *J. Appl. Phys.* 86 (1999) 6239.
- [36] B.A. Gurney et al., *US Patent*, 1999.
- [37] Jiang-Gang Zhu, Youfeng Zheng, G.A. Prinz, *J. Appl. Phys.* 87 (2000) 6668.